

# Intermittent time series forecasting with Gaussian Processes and Tweedie likelihood

Stefano Damato<sup>a,\*</sup>, Dario Azzimonti<sup>a</sup>, Giorgio Corani<sup>a</sup>

<sup>a</sup>*SUPSI, Istituto Dalle Molle di Studi sull'Intelligenza Artificiale (IDSIA), Lugano, Switzerland*

---

## Abstract

We adopt Gaussian Processes (GPs) as latent functions for probabilistic forecasting of intermittent time series. The model is trained in a Bayesian framework that accounts for the uncertainty about the latent function and marginalizes it out when making predictions. We couple the latent GP variable with two types of forecast distributions: the negative binomial (NegBinGP) and the Tweedie distribution (TweedieGP). While the negative binomial has already been used in forecasting intermittent time series, this is the first time in which a fully parameterized Tweedie density is used for intermittent time series. We properly evaluate the Tweedie density, which has both a point mass at zero and heavy tails, avoiding simplifying assumptions made in existing models. We test our models on thousands of intermittent count time series. Results show that our models provide consistently better probabilistic forecasts than the competitors. In particular, TweedieGP obtains the best estimates of the highest quantiles, thus showing that it is more flexible than NegBinGP.

*Keywords:* Intermittent time series, Gaussian Processes, Tweedie distribution, Probabilistic forecasting

---



---

\*Corresponding author

*Email addresses:* `stefano.damato@supsi.ch` (Stefano Damato),  
`dario.azzimonti@supsi.it` (Dario Azzimonti), `giorgio.corani@supsi.ch` (Giorgio Corani)

## 1. Introduction

Intermittent time series characterize a large percentage of the inventory items. Traditional forecasting methods for intermittent demand (Croston, 1972; Syntetos and Boylan, 2005; Nikolopoulos et al., 2011) provide point forecasts only. However, planning the inventory levels requires probability distributions from which to extract the relevant quantiles (Boylan and Syntetos, 2021; Kolassa, 2016).

Probabilistic models for intermittent demand, such as Hyndman et al. (2008, pp.281-283), Snyder et al. (2012), Sbrana (2023), and Svetunkov and Boylan (2023), return the forecast distribution  $p(y_{T+1} \mid y_{1:T})$ , where  $y_{1:T}$  are the observations available up to time  $T$  and  $y_{T+1}$  is the predicted value at time  $T+1$ . Such models predict the distribution of the *demand size* (the positive values of the time series) and the probability of *occurrence*, i.e., the binary variable indicating whether there will be positive demand. They include one or more latent variables, related to the expected value of the demand size or to the probability of occurrence.

The latent variables follow a stochastic process which determines the temporal dynamic of one or more parameters of the forecast distribution. Yet, the above models do not account for the uncertainty about the value of latent variables, which might be substantial. Indeed, incorporating the variability on the parameters of the forecast distribution leads to more reliable forecasts (Prak and Teunter, 2019); this is a typical advantage of the Bayesian approach (Gelman et al., 2020, Chap. 9).

We address the problem by modelling the latent variable with a Gaussian Process (GP), a Bayesian non-parametric model which quantifies the uncertainty of the latent variable and propagates it to the forecast distribution. GPs have been previously applied to smooth time series (Roberts et al., 2013; Corani et al., 2021), but not yet to intermittent time series. Dealing with smooth time series, the GP is generally coupled with a Gaussian forecast distribution. This is however not suitable for intermittent time series, which require a distribution defined over positive values and with a mass in zero, such as the negative binomial (Harvey and Fernandes, 1989; Snyder et al., 2012; Kolassa, 2016). Indeed our first model (NegBinGP) couples the GP with a negative binomial distribution.

The negative binomial is however unimodal; this might be restrictive. The previously mentioned probabilistic models for intermittent time series have a bimodal distribution, with a point mass in zero and a distribution over positive values. Our second model (TweedieGP) couples the GP with a Tweedie (Dunn and Smyth, 2005) distribution, which is a bimodal distribution with a mode in zero and a long right tail.

TweedieGP is the first probabilistic model for intermittent time series based on a fully parameterized Tweedie distribution. As a further contribution we show (Sec. 3.2.1) that the Tweedie loss, often used for training point forecast models on intermittent time series (Jeon and Seong, 2022; Januschowski et al., 2022), is obtained by severely approximating the Tweedie distribution.

We perform experiments on about 40'000 supply chain time series. Both GPs generally provide better probabilistic forecasts than the competitors. In particular, TweedieGP often outperforms the competitors on the highest quantiles, the most important for inventory planning. This might be due to additional flexibility of the Tweedie distribution compared to the negative binomial. Thanks to variational methods (Hensman et al., 2015), the training times of GPs are in line with those of other local models for intermittent time series.

Our implementation is based on GPyTorch (Gardner et al., 2018). Upon acceptance we will publicly release the implementation of our models and of the Tweedie distribution.

## 2. Literature on probabilistic models for intermittent time series

The simplest approach for forecasting intermittent time series is a static model. This is appropriate (Snyder et al., 2012) for time series containing a very large amount of zeros. The static model can be the empirical distribution (Boylan and Syntetos, 2021, Sec 13.2) or a fitted distribution such as the negative binomial (Kolassa, 2016).

In dynamic models, instead, it is common to decompose the intermittent time series into occurrence and demand size. Denoting the observation at time  $t$  as  $y_t$  and the indicator function as  $\mathbb{1}$ , the occurrence and the demand size at time  $t$  are:

$$o_t := \mathbb{1}_{[y_t > 0]},$$

$$d_t := \begin{cases} y_t & \text{if } y_t > 0 \\ \text{undefined} & \text{otherwise} \end{cases}.$$

Thus the values of a time series can be written as  $y_t = o_t \cdot d_t$ .

Several models are based on this decomposition. Croston's method (Croston, 1972), predicts demand sizes and demand intervals with two independent exponential smoothing processes. The TSB method (Teunter et al., 2011) improves by using the second exponential smoothing to predict the occurrence rather than the demand interval. The models of both Croston (1972) and Teunter et al. (2011) return point forecasts only. The probabilistic counterparts of such models have been developed by Hyndman et al. (2008) and Snyder et al. (2012) respectively. The forecast distribution of both models is bimodal, a mixture of a Bernoulli and a shifted Poisson.

Snyder et al. (2012) propose a further model with a single exponential smoothing variable that controls the mean of a negative binomial distribution; in this case the forecast distribution is unimodal and overdispersed.

Sbrana (2023) adopts a latent process which can be equal to 0 with constant probability. The resulting forecast distribution is a mixture of a mass in zero and a truncated Gaussian distribution.

The iETS model (Svetunkov and Boylan, 2023) is possibly the most sophisticated model in this class. It assumes again the independence of occurrence and

demand size and it models the latent variables via exponential smoothing. The latent demand size variable is modelled as a multiplicative exponential smoothing process. iETS considers different models of occurrence, which are based on one or two exponential smoothing processes; they cover cases such as demand building up, demand obsolescence, etc. The best occurrence model is chosen via AICc. The forecast distribution is the mixture of a Bernoulli and a Gamma distribution.

The limit of the above models methods is that they do not account for the uncertainty of the latent processes. Bayesian models (Yelland, 2009; Chapados, 2014; Babai et al., 2021) have been proposed, but there is no public implementation of them.

The WSS method (Willemain et al., 2004) is a non-parametric approach based on the independence between occurrence and demand, which models the occurrence using a two-states Markov chain. When the simulated occurrence is positive, it samples the demand size from past values via bootstrapping with jittering. The forecast distribution is a mixture of a mass in zero and an integer-valued, non-parametric distribution. A limit of WSS is that it does not model the dynamic of the demand size.

It is thus common to independently model occurrence and demand size, which results in a bimodal forecast distribution with a peak mass in zero to model the absence of demand, and a positive mode to describe demand size. However, on sparse time series, the estimate of the demand size is only based on few observations, which can result in large uncertainty.

ADIDA (Nikolopoulos et al., 2011) temporally aggregates the intermittent time series. The aggregated time series are simpler to forecast as they contain fewer zeros. The predictions on aggregated time series, made with the naïve method, are then disaggregated to the original time buckets. ADIDA can be coupled with bootstrapping or conformal inference to produce probabilistic forecasts.

Combinations of point forecasts (Petropoulos and Kourentzes, 2015) and probabilistic forecasts (Wang et al., 2025) have been used to stabilize the performance of above methods. The computational cost is higher, but model selection is not required.

### 3. Gaussian Processes

A Gaussian Process (GP, Rasmussen and Williams, 2006) is a Bayesian method that allows to model the dynamic of a latent variable in a non-parametric fashion. In the Bayesian paradigm, parameters are treated as random variables, initially described by a prior distribution. Uncertainty is then updated based on observed data using Bayes’ theorem, resulting in a posterior distribution. The distribution of the data given the parameters is known as the likelihood (Gelman et al., 2020, Chap. 9). A GP provides a prior distribution on the space of functions  $f : \mathbb{R}_+ \rightarrow \mathbb{R}$ :

$$f \sim \mathcal{GP}(m(\cdot), k(\cdot, \cdot)), \quad (1)$$

where  $m(\cdot)$  is a mean function and  $k(\cdot, \cdot)$  is a positive definite kernel. The prior mean encodes the knowledge we have on the latent function before observing any data. Since we have no prior information we set  $m(t) = c$  for all  $t$ , where  $c \in \mathbb{R}$  is a learnable parameter.

The kernel  $k$  is a positive definite function (Chap. 4, Rasmussen and Williams, 2006) and encodes the covariance between the values of  $f$  at any two instants in time. We assume  $f$  to be a smooth function of time. This assumption is encoded by the Radial Basis Function (RBF) kernel:

$$k(t_i, t_j) = \sigma^2 \exp\left(-\frac{|t_i - t_j|^2}{2\ell^2}\right),$$

where the lengthscale  $\ell \in \mathbb{R}_+$  determines how fast the function changes in time: a smaller  $\ell$  results in quicker variations of  $f$ . The outputscale  $\sigma^2 \in \mathbb{R}_+$  controls the range of values attained by the latent function. Both  $\ell$  and  $\sigma^2$  are learned via optimization; they are referred as kernel hyper-parameters.

By defining a prior directly in the space of functions, GPs do not need regularly spaced observations, therefore we consider a training set of  $T$  couples  $(t_1, y_1), \dots, (t_T, y_T)$ , where, for each  $i$ ,  $t_i$  is the time stamp and  $y_i$  is the observation. We aim to generate forecast for time inputs  $T + 1, \dots, T + h$ , where  $h$  is known as forecast horizon. We denote by  $p$  the density functions. The GP provides a prior on the latent vector  $\mathbf{f}_{1:T} := (f(t_1), \dots, f(t_T))^T$  which, given a set of time instants  $t_1, \dots, t_T$ , encodes the value of the latent function at those times. The prior is a multivariate Gaussian distribution:

$$p(\mathbf{f}_{1:T}) = \mathcal{N}(\mathbf{f}_{1:T} \mid \mathbf{m}_{1:T}, K_{T,T}), \quad (2)$$

where  $\mathbf{m}_{1:T} = (m(t_1), \dots, m(t_T))^T = (c, \dots, c)^T$  and  $K_{T,T} \in \mathbb{R}^{T \times T}$  is the covariance matrix with element  $K_{T,T}(i, j) = k(t_i, t_j)$ .

Samples of vectors  $\mathbf{f}_{1:T}$  are shown in Fig. 1 (left). Credible intervals display the spread of the prior distribution: at time  $t$ , the  $q$ -level *credible interval* is the interval that contains a proportion  $q$  of values of  $f(t)$ . A priori, the function has the same mean and variance at any time; hence the credible intervals are flat (Fig. 1, right).

The latent function  $f$ , defined by the GP prior in eq. (1), is a time-varying parameter related to the mean of the likelihood function, specified here as a negative binomial, (Sec. 3.1) or a Tweedie distribution (Sec. 3.2). For this reason, we require a positive latent function and we ensure this by passing  $f$  through the softplus function, defined as  $\text{softplus}(x) := \log(1 + e^x)$ . The softplus maps negative values of  $x$  to small positive values, while it is close to the identity function for  $x > 2$ . A priori, the credible intervals of  $\text{softplus}(f)$  are identical for all time instants but also non-negative and asymmetric (Fig. 2, left).

Assuming the observations to be conditionally independent given the value of the latent function, the likelihood function is:

$$p(\mathbf{y}_{1:T} \mid \mathbf{f}_{1:T}, \boldsymbol{\theta}_{\text{lik}}) = \prod_{i=1}^T p_{\text{lik}}(y_i \mid \text{softplus}(f_i), \boldsymbol{\theta}_{\text{lik}}), \quad (3)$$

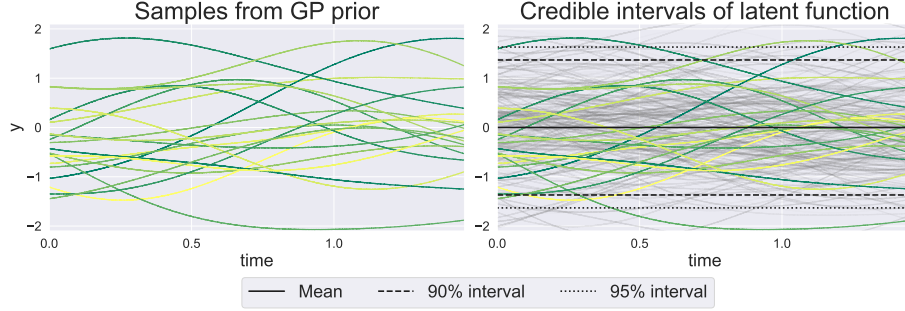


Figure 1: Sample trajectories drawn from the GP prior. The single trajectories fluctuate around the mean, while the credible intervals are flat and symmetric. Samples from  $f$  can be negative.

where  $f_i := f(t_i)$ ,  $p_{\text{lik}}(\cdot \mid \text{softplus}(f_i), \boldsymbol{\theta}_{\text{lik}})$  is either the negative binomial or the Tweedie distribution and  $\boldsymbol{\theta}_{\text{lik}}$  are their hyper-parameters, which we discuss in Secs. 3.1 and 3.2.

After observing the training data, we have residual uncertainty about  $\mathbf{f}_{1:T}$ , described by its posterior distribution:

$$p(\mathbf{f}_{1:T} \mid \mathbf{y}_{1:T}) \propto p(\mathbf{y}_{1:T} \mid \mathbf{f}_{1:T}, \boldsymbol{\theta}_{\text{lik}})p(\mathbf{f}_{1:T}), \quad (4)$$

as shown in the right panel of Fig. 2.

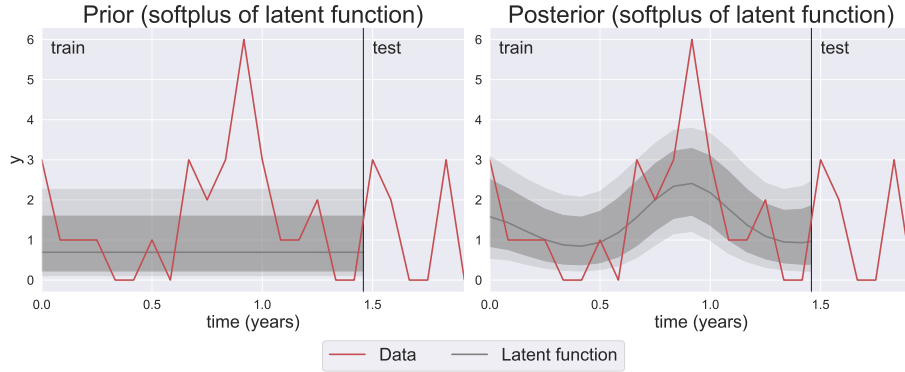


Figure 2: Prior (left) and posterior (right) distribution of the softplus of the GP latent function computed with a Tweedie likelihood. The shaded areas represent the 90% and 95% credible intervals. The vertical line divides train and test data. The data consist of the 1000-th time series from the Auto data set. Fig. 3 (below) shows the prediction intervals for the test data.

The posterior in eq. (4) is available in analytical form only for the Gaussian likelihood. Since our likelihoods are non-Gaussian, we approximate  $p(\mathbf{f}_{1:T} \mid \mathbf{y}_{1:T})$  with a variational inducing point approximation (Hensman et al., 2013) constituted by a Gaussian density, denoted by  $q(\mathbf{f}_{1:T} \mid \mathbf{y}_{1:T})$ , with tunable mean and

covariance parameters. We follow Hensman et al. (2015) to optimize the model parameters as described in Appendix A. In what follows we denote the fitted variational approximation by  $q(\mathbf{f}_{1:T} | \mathbf{y}_{1:T})$ .

The distribution of the future values of the latent function,  $\mathbf{f}_{T+1:T+h} = (f(t_{T+1}), \dots, f(t_{T+h}))^\top$ , is:

$$p(\mathbf{f}_{T+1:T+h} | \mathbf{y}_{1:T}) = \int p(\mathbf{f}_{T+1:T+h} | \mathbf{f}_{1:T}) q(\mathbf{f}_{1:T} | \mathbf{y}_{1:T}) d\mathbf{f}_{1:T}, \quad (5)$$

where the integral is solved analytically since both  $p$  and  $q$  are Gaussian.

We obtain the forecast distribution by sampling from  $p(\mathbf{f}_{T+1:T+h} | \mathbf{y}_{1:T})$  and passing each sample through the likelihood. Thus the uncertainty on  $\mathbf{f}_{T+1:T+h}$  is propagated to the forecast distribution  $p(\mathbf{y}_{T+1:T+h} | \mathbf{y}_{1:T})$ . Fig. 3 shows the posterior distribution of  $\mathbf{f}_{T+1:T+h}$  (left) and the forecast distribution (right).

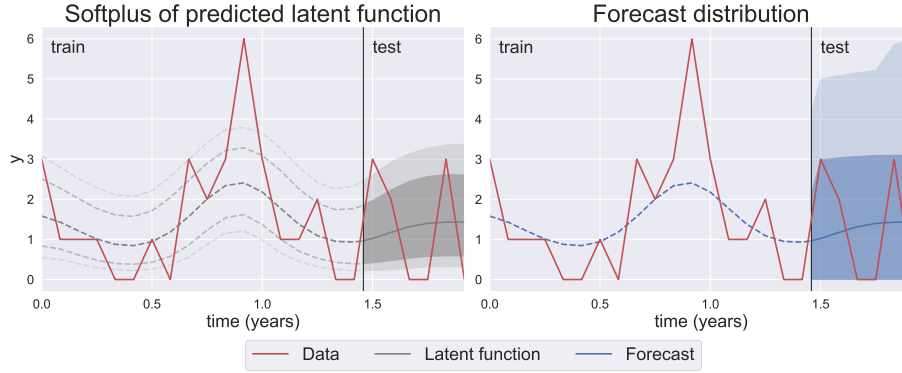


Figure 3: Example of TweedieGP forecasting. Left: posterior distribution of the GP latent function passed through the softplus. Right: forecast distribution using the Tweedie likelihood. The shaded regions represents 90% and 95% prediction intervals respectively. The figures complement the model fit in Fig. 2.

The distribution of the latent function at future times, shown in eq. (5), is obtained marginalizing a multivariate Gaussian distribution. Given a likelihood expressed as in eq. (3),  $h$ -steps ahead forecasts are obtained without autoregressive sampling. We now complete the GP model by specifying the likelihood function.

### 3.1. Negative binomial likelihood

The negative binomial distribution can model intermittent demand (Snyder et al., 2012; Kolassa, 2016), since it can have both a large probability mass in zero and long tails.

We denote by  $\text{NegBin}(y; r, p)$  the density of a negative binomial distribution;  $r$  is the number of successes and  $p$  denotes, with a slight abuse of notation, the success probability. The mean and the variance of the distribution linearly increase with  $r$ ;  $p$  controls the overdispersion. We model  $r$  through the GP,

by setting  $r = \text{softplus}(f)$ . Instead, we treat  $p$  as a learnable hyper-parameter ( $\theta_{\text{lik}} = \{p\}$ ) which we keep fixed for all the data points of the same time series.

The likelihood of an observation  $y_i$  is:

$$p_{\text{lik}}(y_i \mid \text{softplus}(f_i), \theta_{\text{lik}}) = \text{NegBin}(y_i; \text{softplus}(f_i), p).$$

We obtain NegBinGP by plugging this likelihood in eq. (3) and by following the procedure in the previous section.

### 3.2. The Tweedie likelihood

The Tweedie is a family of exponential dispersion models (a generalization of the exponential family, see Dunn and Smyth, 2005) characterized by a power mean-variance relationship. A non-negative random variable  $Y$  is distributed as a Tweedie,  $Y \sim \text{Tw}(\mu, \phi, \rho)$ , if  $Y$  follows an exponential dispersion model distribution such that

$$\text{Var}[Y] = \phi \mu^\rho,$$

where  $\mu > 0$  is the mean,  $\rho > 0$  is the *power* and  $\phi > 0$  is the *dispersion* parameter.

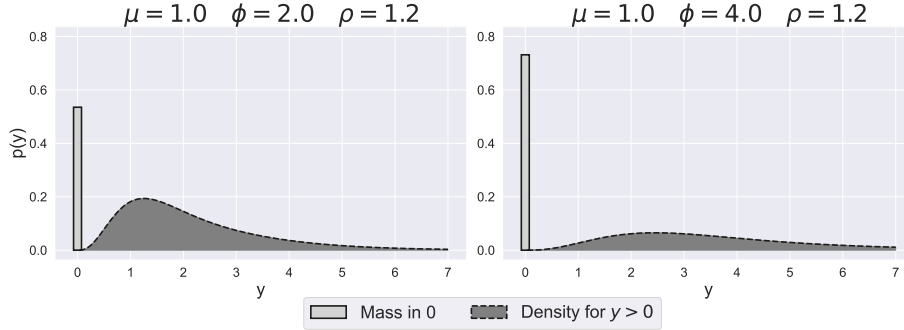


Figure 4: The Tweedie distribution is flexible and possibly bimodal. The two distributions have the same mean, but the right one has higher dispersion ( $\phi$ ), implying a larger mass in 0 and in a longer right tail.

Depending on  $\rho$ , the Tweedie family includes the Gaussian ( $\rho = 0$ ), Poisson ( $\rho = 1$ ), and Gamma ( $\rho = 2$ ) distributions. However, we restrict  $\rho \in (1, 2)$  to have a non-negative distribution with a possible point mass in zero. In this setting the Tweedie (Dunn and Smyth, 2005) is a Poisson mixture of Gamma distributions:

$$\begin{aligned} Y &\sim \sum_{i=0}^N X_i, \\ X_i &\stackrel{\text{i.i.d.}}{\sim} \text{Gamma}(\alpha, \beta), \\ N &\sim \text{Poisson}(\lambda), \end{aligned}$$



with

$$\lambda = \frac{\mu^{2-\rho}}{\phi(2-\rho)}, \quad \alpha = \frac{2-\rho}{\rho-1}, \quad \beta = \frac{1}{\phi(\rho-1)\mu^{\rho-1}}. \quad (6)$$

The mass in 0 and the density for  $y > 0$  are:

$$\mathbb{P}(Y = 0) = \mathbb{P}(N = 0) = e^{-\lambda}, \quad (7)$$

$$p(y \mid \lambda, \alpha, \beta) = \sum_{n=1}^{+\infty} e^{-\lambda} \frac{\lambda^n}{n!} \cdot \text{Ga}(y \mid n \cdot \alpha, \beta), \quad (8)$$

where  $\mathbb{P}$  denotes the probability of an event and  $\text{Ga}(\cdot)$  is the density of a Gamma distribution. The Tweedie distribution is generally bimodal (Fig. 4): the first mode is in 0, while the second one is the mode of the mixture of Gamma distributions. This mixture has a continuous density function on the positive real values. Count forecasts can be generated by rounding the samples.

The parametrization (7-8), though interpretable, is not usable as a likelihood function. Indeed there is no theoretical result for truncating the infinite sum in eq. (8) while controlling the exceedance probability. In order to evaluate the Tweedie we use the  $(\mu, \phi, \rho)$  parametrization (Dunn and Smyth, 2005). The probability of zero and the continuous density for  $y > 0$  are:

$$\mathbb{P}(Y = 0) = \exp\left(-\frac{\mu^{2-\rho}}{\phi(2-\rho)}\right), \quad (9)$$

$$p(y \mid \mu, \phi, \rho) = A(y) \cdot \exp\left[\frac{1}{\phi} \left(y \frac{\mu^{1-\rho}}{1-\rho} - \frac{\mu^{2-\rho}}{2-\rho}\right)\right], \quad (10)$$

with

$$\begin{aligned} A(y) &= \frac{1}{y} \sum_{j=1}^{\infty} \frac{y^{j\alpha} (\rho-1)^{-j\alpha}}{\phi^{j(1+\alpha)} (2-\rho)^j j! \Gamma(j\alpha)} \\ &= \frac{1}{y} \sum_{j=1}^{\infty} V(j), \end{aligned} \quad (11)$$

where  $\alpha$  is defined in eq. (6). Dunn and Smyth (2005) provide a truncating rule for evaluating the infinite summation of eq. (11). It exploits the fact that  $V(j)$  is a concave function of  $j$ . In Appendix B.1 we report the derivations of the truncating rule and we show that we generally require less than 10 terms in the summation of eq. (11) for a precise approximations. The Tweedie density is complex to implement; yet, its evaluation only requires a small overhead compared to other distributions.

The likelihood of TweedieGP is thus obtained by substituting in eq. (3):

$$p_{\text{lik}}(y_i \mid \text{softplus}(f_i), \boldsymbol{\theta}_{\text{lik}}) = \text{Tw}(y_i; \text{softplus}(f_i), \phi, \rho),$$

where  $\boldsymbol{\theta}_{\text{lik}} = \{\phi, \rho\}$ . We set  $\mu = \text{softplus}(f)$ . Thus the latent variable affects, through  $\lambda$  and  $\beta$ , both the mass in 0 and the distribution on the positive  $y$ , see

eq. (6), (7), (8). We thus control a bimodal forecast distribution using a single latent process. The hyper-parameters  $\phi$  and  $\rho$  are optimized and they are equal for all the data points in the same time series.

We now discuss the relation between the Tweedie distribution and the Tweedie loss, often used to train point forecast models on intermittent time series.

### 3.2.1. Comparison with Tweedie loss

Januschowski et al. (2022) mention the *Tweedie loss* for tree-based models as one of the reasons of success in the M5 competition. Also Jeon and Seong (2022) obtained good results in the M5 competition by training a DeepAR (Salinas et al., 2020) with the Tweedie loss. The Tweedie loss is indeed available both in `lightGBM`<sup>1</sup> and in `PyTorch Forecasting`<sup>2</sup>. But such models only return point forecasts. We clarify, for the first time, that the Tweedie loss is obtained from the Tweedie distribution via a rough approximation, which makes it unsuitable for probabilistic forecasting.

The Tweedie loss (Jeon and Seong, 2022) is:

$$\mathcal{L}(\mu, \rho | y) = -y \frac{\mu^{1-\rho}}{1-\rho} + \frac{\mu^{2-\rho}}{2-\rho}. \quad (12)$$

Interpreting eq. (12) as a negative log-likelihood, the implied likelihood is:

$$p(y | \mu, \rho) = \exp \left( y \frac{\mu^{1-\rho}}{1-\rho} - \frac{\mu^{2-\rho}}{2-\rho} \right), \quad (13)$$

which approximates the Tweedie density in eq. (10) by setting both  $A(y) = 1$  and  $\phi = 1$ . Setting  $A(y) = 1$  for all  $y > 0$  avoids evaluating the infinite summation in eq. (11); however, this makes the distribution unimodal and shortens its tails. Indeed,  $A$  is a function of  $y$  and not a simple normalization constant. Moreover, fixing the dispersion parameter to  $\phi = 1$  further reduces the flexibility. In Sec. 4.6 we show that the accuracy of TweedieGP worsens when we adopt the approximation with  $A(y) = 1$ ,  $\phi = 1$  rather than the actual Tweedie distribution.

We can nevertheless understand why the function in eq. (12) is an effective loss function for point forecast on intermittent time series. The first term of the exponential corresponds to an unnormalised exponential distribution and the second term is a penalty term which forces  $\mu$  to remain close to zero. We illustrate the shape of the unnormalized distribution from eq. (13) in Appendix B.2.

## 4. Experiments

We consider a time series as intermittent (Syntetos et al., 2005) if the average demand interval (ADI) is larger than 1.32. By applying this criterion, we extract

<sup>1</sup><https://lightgbm.readthedocs.io/en/latest/Parameters.html>

<sup>2</sup>[https://pytorch-forecasting.readthedocs.io/en/stable/api/pytorch\\_forecasting\\_metrics.point.TweedieLoss.html](https://pytorch-forecasting.readthedocs.io/en/stable/api/pytorch_forecasting_metrics.point.TweedieLoss.html)

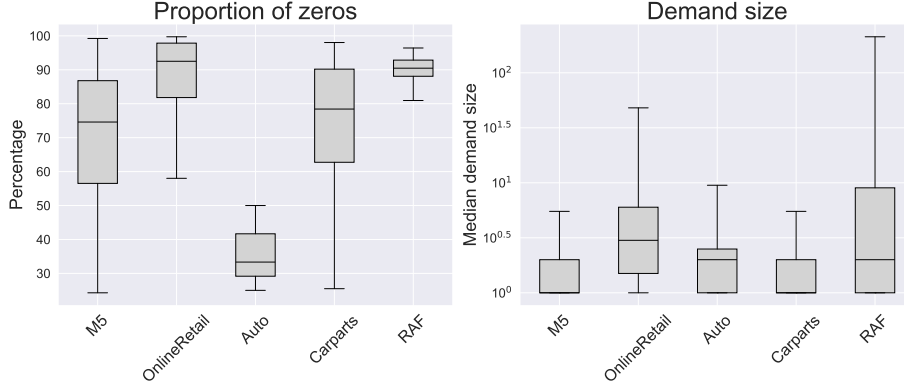


Figure 5: Proportion of zeros and median demand size in the different data sets; the y-axis of the median demand size is in  $\log_{10}$  scale.

| Name         | # of t.s. | Freq    | $T$  | $h$ |
|--------------|-----------|---------|------|-----|
| M5           | 29003     | Daily   | 1941 | 28  |
| OnlineRetail | 2023      | Daily   | 333  | 31  |
| Auto         | 1227      | Monthly | 18   | 6   |
| Carparts     | 2499      | Monthly | 45   | 6   |
| RAF          | 5000      | Monthly | 72   | 12  |

Table 1: Characteristics of the extracted intermittent time series. The data sets are from these domains: in-store sales, online sales, spare parts supply for cars and aircrafts.

about 40'000 intermittent time series from the five data sets of Tab. 1.  $T$  is the length of the training data, and  $h$  is the forecast horizon used in the experiments. We show in Fig. 5 how the proportion of zeros and the demand size varies across the time series of each data set.

The data sets with the highest proportion of zeros (median 0.9) are RAF and OnlineRetail (Fig. 5 left). However, the time series of OnlineRetail are about five times longer than those of RAF, Tab. 1. In contrast, Auto has the lowest proportion of zeros (median 0.35) and its time series are also the shortest ( $T = 18$ ). The M5 data set is the most heterogeneous as for proportion of zeros and it generally has narrow demand size. It also contains the largest amount (29'003) of time series, which are also very long ( $T = 1941$ ). In Appendix C we report the source of each data set.

#### 4.1. GP training

We implement our models in GPyTorch (Gardner et al., 2018). We estimate the variational parameters, the hyper-parameters of the GP ( $c, \ell, \sigma^2$ ) and of the likelihood ( $p$  for the negative binomial distribution,  $\phi$  and  $\rho$  for the Tweedie) via gradient descent for 100 iterations with early stopping, using Adam optimizer (Kingma and Ba, 2017) with learning rate 0.1.

We train a GP for each time series. For both NegBinGP and TweedieGP, we obtain the forecast distribution by drawing 50'000 samples. Training and prediction times are of the same order of magnitude of iETS, as detailed in Sec. 4.5. Rarely, the training fails due to numerical issues; when this happens, we restart the optimization.

Before training TweedieGP, we scale the observations by dividing them by the median demand size, that is, we divide each value by  $\text{median}(\{y_i : y_i > 0, i = 1, \dots, T\})$ ; this simplifies the optimization. This scaling can be applied as the zeroes remain unchanged and the Tweedie distribution is absolutely continuous on positive data. We bring the samples back to the original scale after drawing them. We evaluate the effect of the scaling in Sec. 4.6.

#### 4.2. Baselines

We compare NegBinGP and TweedieGP against empirical quantiles (EmpQuant), WSS, ADIDA<sub>C</sub>, and iETS. We implemented on our own WSS (Willemain et al., 2004), drawing 50'000 samples from its forecast distribution.

We use ADIDA (Nikolopoulos et al., 2011) generating prediction intervals via conformal inference (Angelopoulos and Bates, 2023), using the implementation provided by `statsforecast` (Garza et al., 2022). We refer to it as ADIDA<sub>C</sub>, where the subscript stands for conformal.

We use iETS (Svetunkov and Boylan, 2023) from the `smooth` package (Svetunkov (2024), v. 4.1.1). We use the most complete model (iETS<sub>A</sub>) which fits four different occurrence models and selects among them via AICc. We draw 50'000 samples from the forecast distribution.

In Appendix C, we show how to reproduce our experiments and we detail the integration of our models in GPyTorch (Gardner et al., 2018).

#### 4.3. Metrics

Denoting by  $\hat{y}^q$  the forecast of quantile  $q$ , and by  $y$  the observed value, the quantile loss (Gneiting and Raftery, 2007) is:

$$Q_q(\hat{y}^q, y) = 2 \cdot \begin{cases} q(y - \hat{y}^q) & \text{if } y \geq \hat{y}^q \\ (1 - q)(\hat{y}^q - y) & \text{else} \end{cases}. \quad (14)$$

For high quantiles  $q$ , this metric strongly penalises cases in which  $y$  exceeds the predicted value  $\hat{y}^q$ , that is, when the demand size is underestimated. We evaluate  $Q_q(\hat{y}^q, y)$  for the quantile levels  $q \in \{0.5, 0.8, 0.9, 0.95, 0.99\}$ . We do not assess quantiles lower than 0.5 because they are generally zero for all models.

The quantile loss is however scale-dependent. In order to obtain a scale-free indicator (Athanasopoulos and Kourentzes, 2023) we scale it by the quantile loss of the empirical quantiles ( $\text{emp}^q$ ) on the training data, and we average it through the forecast horizon. Let  $\hat{\mathbf{y}}_{T+1:T+h}^q := (\hat{y}_{T+1}^q, \dots, \hat{y}_{T+h}^q)^\top$  be the forecasts of quantile  $q$  from times  $T + 1$  to  $T + h$ ; the scaled quantile loss is:

$$\text{s}Q_q(\hat{\mathbf{y}}_{T+1:T+h}^q, \mathbf{y}_{T+1:T+h}) = \frac{\frac{1}{h} \sum_{t=1}^h Q_q(\hat{y}_{T+t}^q, y_{T+t})}{\frac{1}{T} \sum_{t=1}^T Q_q(\text{emp}^q, y_t)}.$$

The values of  $sQ_q$  are usually greater than 1 since the scaling factor, based on the training set, is optimistically biased.

The scaled quantile loss scores the quantile predictions as point forecasts. We then assess the entire predictive distribution, using an indicator similar to the Ranked Probability Score (RPS, Czado et al., 2009). The RPS can be approximated by averaging the quantile loss computed for multiple probability levels (Bracher et al., 2021). For many applications involving intermittent time series, the lower part of the forecast distribution is not relevant (Boylan and Syntetos, 2006). We thus focus on a set of probability levels  $L = \{0.5, 0.55, 0.6, 0.65, 0.7, 0.75, 0.8, 0.85, 0.9, 0.95, 0.99\}$  with cardinality  $|L|$  and we propose the metric

$$\text{RPS}_{0.5+}(\{\hat{y}^q\}^{q \in L}, y) = \frac{1}{|L|} \sum_{q \in L} Q_q(\hat{y}^q, y),$$

where the subscript shows that we only consider quantiles equal to or greater than 0.5. We make it scale-independent by scaling it by  $\text{RPS}_{0.5+}$  of the empirical quantiles:

$$\text{SRPS}_{0.5+}(\{\hat{\mathbf{y}}_{T+1:T+h}^q\}^{q \in L}, \mathbf{y}_{T+1:T+h}) = \frac{\frac{1}{h} \sum_{t=1}^h \text{RPS}_{0.5+}(\{\hat{y}_{T+t}^q\}^{q \in L}, y_{T+t})}{\frac{1}{T} \sum_{t=1}^T \text{RPS}_{0.5+}(\{\text{emp}^q\}^{q \in L}, y_t)}.$$

We also report the Root Mean Squared Scaled Error (RMSSE) (Hyndman and Koehler, 2006) of the point forecasts:

$$\text{RMSSE}(\hat{\mathbf{y}}_{T+1:T+h}, \mathbf{y}_{T+1:T+h}) = \sqrt{\frac{\frac{1}{h} \sum_{t=1}^h (\hat{y}_{T+t} - y_{T+t})^2}{\frac{1}{T-1} \sum_{t=2}^T (y_t - y_{t-1})^2}}$$

where  $\hat{\mathbf{y}}_{T+1:T+h} := (\hat{y}_{T+1}, \dots, \hat{y}_{T+h})^\top$  denotes a vector of forecasts. We use the mean of the forecast distribution as point forecast, as this is the minimizer of RMSSE (Kolassa, 2020).

Finally, we measure the forecast coverage, i.e., the proportion of observations that lie within the  $q$ -level prediction interval. An ideal forecast has coverage  $q$ . However, for discrete data concentrated around low values, actual quantiles exist only at a coarse probability level; for instance we might have  $\hat{y}^{0.2} = \hat{y}^{0.5} = 0$ .

#### 4.4. Discussion

We show in Tab. 2 the score of each method, averaged with respect to all the time series of each data set. In each row, we boldface the model with the lowest average loss and the models whose average loss is not significantly different from the best. We test significance of the difference in loss by using the paired  $t$ -test with FDR correction for multiple comparisons (Hastie et al., 2009, Sec 18.7.1).

We argue that the mean of the quantile losses, and not a rank-based statistic, should be analyzed. The distribution of the quantile loss is strongly asymmetric: most forecasts have a small quantile loss; only a few forecasts incur a large

| Data set     | Metric               | EmpQuant    | WSS         | ADIDA <sub>C</sub> | iETS        | NegBinGP    | TweedieGP   |
|--------------|----------------------|-------------|-------------|--------------------|-------------|-------------|-------------|
| M5           | sQ <sub>0.5</sub>    | 1.88        | 1.87        | 1.88               | 1.83        | <b>1.78</b> | 1.79        |
|              | sQ <sub>0.8</sub>    | 1.74        | 1.77        | <b>1.46</b>        | 1.65        | 1.48        | <b>1.46</b> |
|              | sQ <sub>0.9</sub>    | 1.57        | 1.65        | 1.35               | 1.56        | 1.29        | <b>1.26</b> |
|              | sQ <sub>0.95</sub>   | 1.39        | 1.51        | 1.37               | 1.60        | 1.19        | <b>1.16</b> |
|              | sQ <sub>0.99</sub>   | 1.25        | 1.40        | 1.69               | 2.25        | <b>1.16</b> | <b>1.16</b> |
|              | SRPS <sub>0.5+</sub> | 1.73        | 1.75        | 1.57               | 1.71        | 1.51        | <b>1.50</b> |
|              | RMSSE                | 0.98        | 1.00        | <b>0.94</b>        | <b>0.94</b> | <b>0.94</b> | <b>0.94</b> |
| OnlineRetail | sQ <sub>0.5</sub>    | 2.35        | 2.35        | 2.55               | 2.36        | <b>2.34</b> | 2.35        |
|              | sQ <sub>0.8</sub>    | 2.34        | 2.33        | 2.29               | 2.40        | <b>2.27</b> | <b>2.26</b> |
|              | sQ <sub>0.9</sub>    | 2.31        | 2.29        | 2.23               | 2.51        | 2.23        | <b>2.20</b> |
|              | sQ <sub>0.95</sub>   | 2.33        | 2.30        | 2.35               | 2.75        | 2.25        | <b>2.23</b> |
|              | sQ <sub>0.99</sub>   | 3.02        | <b>2.98</b> | 4.09               | 4.36        | 3.22        | <b>2.98</b> |
|              | SRPS <sub>0.5+</sub> | 2.36        | 2.35        | 2.44               | 2.51        | 2.32        | <b>2.30</b> |
|              | RMSSE                | 0.97        | 0.98        | <b>0.94</b>        | <b>0.94</b> | <b>0.94</b> | 0.95        |
| Auto         | sQ <sub>0.5</sub>    | 1.15        | 1.36        | 1.19               | 1.17        | <b>1.14</b> | <b>1.14</b> |
|              | sQ <sub>0.8</sub>    | 1.30        | 1.53        | 1.34               | 1.39        | 1.29        | <b>1.28</b> |
|              | sQ <sub>0.9</sub>    | 1.48        | 1.65        | 1.59               | 1.54        | <b>1.42</b> | <b>1.42</b> |
|              | sQ <sub>0.95</sub>   | 1.84        | 1.84        | 2.21               | 1.76        | 1.65        | <b>1.62</b> |
|              | sQ <sub>0.99</sub>   | 4.32        | 2.57        | 7.51               | 3.28        | <b>2.45</b> | 2.56        |
|              | SRPS <sub>0.5+</sub> | 1.26        | 1.47        | 1.37               | 1.31        | <b>1.23</b> | 1.24        |
|              | RMSSE                | <b>0.78</b> | 0.91        | 0.79               | <b>0.78</b> | <b>0.78</b> | <b>0.78</b> |
| Carparts     | sQ <sub>0.5</sub>    | 1.13        | 1.15        | 1.20               | <b>1.10</b> | <b>1.10</b> | 1.11        |
|              | sQ <sub>0.8</sub>    | 1.18        | 1.33        | 1.14               | 1.15        | <b>1.10</b> | <b>1.09</b> |
|              | sQ <sub>0.9</sub>    | 1.25        | 1.45        | 1.16               | 1.24        | 1.16        | <b>1.13</b> |
|              | sQ <sub>0.95</sub>   | 1.32        | 1.63        | 1.34               | 1.46        | <b>1.17</b> | 1.19        |
|              | sQ <sub>0.99</sub>   | 1.86        | 1.99        | 3.72               | 3.04        | 1.65        | <b>1.56</b> |
|              | SRPS <sub>0.5+</sub> | 1.19        | 1.29        | 1.25               | 1.18        | <b>1.10</b> | <b>1.10</b> |
|              | RMSSE                | 0.66        | 0.78        | 0.60               | <b>0.59</b> | 0.61        | 0.61        |
| RAF          | sQ <sub>0.5</sub>    | <b>1.00</b> | <b>1.00</b> | 1.37               | <b>1.00</b> | <b>1.00</b> | <b>1.00</b> |
|              | sQ <sub>0.8</sub>    | <b>1.00</b> | 1.01        | 1.22               | <b>1.00</b> | 1.01        | 1.01        |
|              | sQ <sub>0.9</sub>    | 1.10        | 1.16        | 1.17               | <b>1.07</b> | 1.12        | 1.14        |
|              | sQ <sub>0.95</sub>   | <b>1.24</b> | 1.43        | 1.35               | 1.38        | <b>1.24</b> | 1.26        |
|              | sQ <sub>0.99</sub>   | 2.12        | 2.21        | 3.79               | 3.89        | 2.21        | <b>2.09</b> |
|              | SRPS <sub>0.5+</sub> | <b>1.06</b> | 1.09        | 1.38               | 1.12        | 1.07        | 1.08        |
|              | RMSSE                | 0.61        | 0.65        | 0.61               | <b>0.59</b> | 0.60        | 0.60        |

Table 2: Metrics averaged over the time series of each data set.

loss. The mean is sensitive to such rare and large losses, unlike rank statistics. Moreover, the correct predictive distribution is guaranteed to minimize the expected value of the scoring rule (Gneiting and Raftery, 2007), but there are no guarantees for rank statistics.

TweedieGP is often the best performing model on the highest quantiles  $\{0.9, 0.95, 0.99\}$ , the most important for decision making. This might be due to Tweedie distribution’s ability to extend its tails.

TweedieGP and NegBinGP perform similarly on data sets containing short time series (Auto, Carparts, RAF), where the effect of the GP prior might be more important than the choice of the likelihood. In contrast, on data sets containing longer time series (OnlineRetail, M5), TweedieGP has generally an advantage over NegBinGP. The advantage of TweedieGP on the highest quantiles is emphasized on OnlineRetail, whose time series are both long and with high demand sizes (see Fig. 5), challenging the long tail of the forecast distribution.

iETS is a good match for the GP models on the lowest quantile we consider, but it is generally outperformed on the highest quantiles. Also in Svetunkov and Boylan (2023), iETS is outperformed by other methods on the the average quantile loss.

The empirical quantiles are generally preferable to both WSS and ADIDA<sub>C</sub>. In particular on the RAF data set, which is characterized by the largest amount of zeros, the empirical quantiles match the performance of the GPs. This confirms the suitability of static models for very sparse time series; it also shows that the GP model adapts well to different types of temporal correlations, becoming an i.i.d. model when needed.

The results of the approximate RPS are in line with those of the individual quantiles. The best models according to RMSSE are iETS, ADIDA<sub>C</sub>, and GPs. The differences observed between these methods are often very small. However, ADIDA<sub>C</sub> performs poorly on the quantile loss, showing that conformal inference is currently unsuitable for probabilistic forecasting on count data.

Fig. 6 shows the calibration of selected methods (empirical quantiles, iETS and TweedieGP) on three data sets (Auto, M5 and RAF) containing respectively the shortest, longest and most sparse time series. Better forecasts lie closer to the dotted diagonal line. On intermittent time series, the coverage is at least as large as the proportion of zeros; there is hence overcoverage of the lower quantiles, as clear from the third panel of Fig. 6. Indeed, for a discrete variable that is concentrated around low values, meaningful quantiles only exist for high enough probability level; e.g., a forecast of quantile 0.5 may in fact be a forecast of quantile 0.8.

On the Auto data set, which has moderate intermittency, only TweedieGP has almost correct coverage on all quantiles above 0.5. A similar comment can be done for M5, even though in this case the proportion of zeros is larger. Correct coverage is provided, only by TweedieGP and empirical quantiles, for quantiles above 0.8. On the RAF data set, the very sporadic positive demand implies forecast overcoverage apart from the highest quantiles.

It is also interesting to analyze how the models compare on the quantile loss

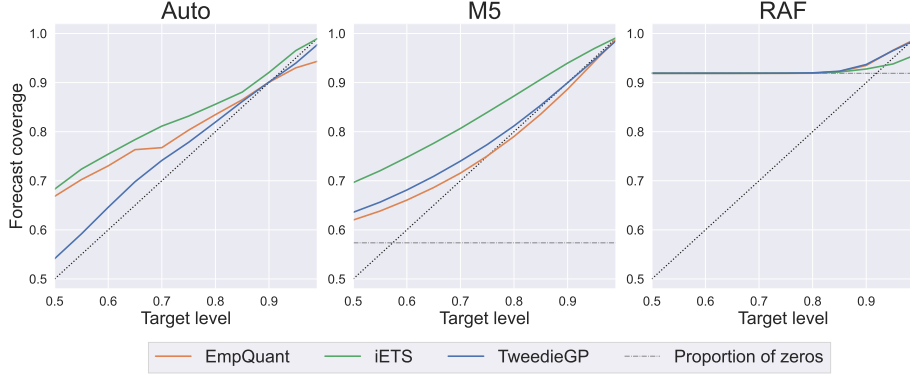


Figure 6: The coverage cannot go below the proportion of zeros in the test set, shown by a dashed horizontal line. On RAF, this implies overcoverage of most quantiles, apart from the highest ones.

when they are correctly calibrated. For instance, empirical quantiles, iETS and TweedieGP provide correct coverage on the 95-th percentile of M5. On Auto, both TweedieGP and the empirical quantiles provide correct coverage on quantile 0.9. In these cases, TweedieGP provides the lowest quantile loss (Tab. 2) among correctly calibrated models. Recall that the quantile loss combines a reward for the sharpness and a miscoverage penalty. Hence, given the same calibration, TweedieGP achieves lower loss as it provides a sharper estimate of the quantiles.

#### 4.5. Computational times

| Data set     | WSS             | ADIDA <sub>C</sub> | iETS            | NegBinGP        | TweedieGP       |
|--------------|-----------------|--------------------|-----------------|-----------------|-----------------|
| M5           | $0.10 \pm 0.03$ | $0.01 \pm 0.01$    | $0.76 \pm 0.07$ | $1.20 \pm 0.39$ | $2.12 \pm 0.49$ |
| OnlineRetail | $0.11 \pm 0.05$ | $0.01 \pm 0.01$    | $0.44 \pm 0.06$ | $0.32 \pm 0.18$ | $0.35 \pm 0.22$ |
| Auto         | $0.04 \pm 0.02$ | $0.01 \pm 0.01$    | $0.13 \pm 0.03$ | $0.20 \pm 0.06$ | $0.20 \pm 0.08$ |
| Carparts     | $0.05 \pm 0.02$ | $0.01 \pm 0.01$    | $0.14 \pm 0.03$ | $0.17 \pm 0.11$ | $0.24 \pm 0.12$ |
| RAF          | $0.05 \pm 0.03$ | $0.01 \pm 0.01$    | $0.20 \pm 0.03$ | $0.22 \pm 0.06$ | $0.30 \pm 0.07$ |

Table 3: Mean and standard deviation of the time (seconds) for training the models and generating forecasts. Experiments are run on the CPU of a M3 MacBook Pro.

We report in Tab. 3 the computational times per time series of each method, including training and generating the forecasts on time series each data set. Empirical quantiles are practically immediate and their execution times are not shown in the table ADIDA<sub>C</sub> and WSS are the fastest methods.

The computational time of our GPs is comparable with that of iETS. On the data sets containing the longest time series (M5), the average computational time of the GPs is about 2 seconds. An exact GP implementation would



be rather slow on the time series of the M5 data set, due to its cubic computational complexity in the number of observations  $T$ . Thanks to the variational approximation, the computational complexity of our models is instead quadratic in  $T$  for  $T < 200$ . For longer time series the cost is capped by the variational formulation and becomes linear in  $T$ . See Appendix A for a more detailed evaluation.

The computational times of TweedieGP and NegBinGP are close; the fully parameterised Tweedie density only implies a small overhead compared to the negative binomial, which is simple to evaluate. On the M5 data set, NegBinGP is faster than TweedieGP as it often meets the early stopping condition.

#### 4.6. Ablation study

We compare TweedieGP against a GP model trained with the approximate Tweedie likelihood with  $A(y) = \phi = 1$  (implied by the Tweedie loss) and a TweedieGP trained with no scaling. We keep the same experimental setup of the previous section and we show the results in Tab. 4.

The accuracy of TweedieGP worsens on unscaled data. Due to numerical issues, the posterior mean of the Gaussian process does not grow over a certain value, which is problematic when demand sizes become high.

Finally, the performance of the approximated Tweedie likelihood with  $\phi = A = 1$  confirms what discussed in Sec. 3.2.1: the Tweedie loss might produce effective point forecasts by penalizing values far from zero, but the shorter tails negatively affect the estimate of the higher quantiles.

## 5. Conclusions

The prediction of intermittent time series should be based on probability distributions rather than on point forecasts. The most common probabilistic models are based on a latent variable related to the demand size and to the probability of occurrence. This paper proposes to model such a latent variable with a Gaussian Process, which quantifies the uncertainty on the latent variable and propagates it into the forecast distribution, thus obtaining more reliable prediction intervals.

We test two variants of GP with different likelihoods: the negative binomial and the Tweedie. The two models perform similarly, but TweedieGP performs better on the high quantiles. Our model is the first probabilistic model for intermittent time series which adopts the Tweedie likelihood, which is flexible but whose density is difficult to evaluate. Hence we find it useful to publicly release the Tweedie likelihood, making it possible to train novel models probabilistic models for intermittent time series in the future.

In our models, only one of the forecast distribution parameters varies over time. The others are estimated once for each time series. More complex GP models, such as Chained GPs (Saul et al., 2016), could be used to dynamically model two or more parameters, possibly creating a global model, i.e. a model that simultaneously learns all the series of a data set. We leave however the

| Data set     | Metric               | No scaling  | $A(y) = \phi = 1$ | TweedieGP   |
|--------------|----------------------|-------------|-------------------|-------------|
| M5           | sQ <sub>0.5</sub>    | <b>1.79</b> | 1.80              | <b>1.79</b> |
|              | sQ <sub>0.8</sub>    | <b>1.46</b> | 1.47              | <b>1.46</b> |
|              | sQ <sub>0.9</sub>    | 1.27        | 1.30              | <b>1.26</b> |
|              | sQ <sub>0.95</sub>   | 1.17        | 1.23              | <b>1.16</b> |
|              | sQ <sub>0.99</sub>   | 1.17        | 1.37              | <b>1.16</b> |
|              | SRPS <sub>0.5+</sub> | <b>1.50</b> | 1.52              | <b>1.50</b> |
|              | RMSSE                | <b>0.94</b> | <b>0.94</b>       | <b>0.94</b> |
| OnlineRetail | sQ <sub>0.5</sub>    | <b>2.35</b> | 2.43              | <b>2.35</b> |
|              | sQ <sub>0.8</sub>    | 2.29        | 2.31              | <b>2.26</b> |
|              | sQ <sub>0.9</sub>    | 2.26        | 2.25              | <b>2.20</b> |
|              | sQ <sub>0.95</sub>   | 2.35        | 2.31              | <b>2.23</b> |
|              | sQ <sub>0.99</sub>   | 3.39        | 3.42              | <b>2.98</b> |
|              | SRPS <sub>0.5+</sub> | 2.35        | 2.38              | <b>2.30</b> |
|              | RMSSE                | <b>0.95</b> | <b>0.95</b>       | <b>0.95</b> |
| Auto         | sQ <sub>0.5</sub>    | <b>1.15</b> | <b>1.13</b>       | <b>1.14</b> |
|              | sQ <sub>0.8</sub>    | <b>1.28</b> | 1.30              | <b>1.28</b> |
|              | sQ <sub>0.9</sub>    | 1.43        | 1.44              | <b>1.42</b> |
|              | sQ <sub>0.95</sub>   | 1.66        | 1.65              | <b>1.62</b> |
|              | sQ <sub>0.99</sub>   | 2.80        | 2.58              | <b>2.56</b> |
|              | SRPS <sub>0.5+</sub> | <b>1.24</b> | <b>1.24</b>       | <b>1.24</b> |
|              | RMSSE                | <b>0.78</b> | <b>0.78</b>       | <b>0.78</b> |
| Carparts     | sQ <sub>0.5</sub>    | <b>1.10</b> | 1.11              | 1.11        |
|              | sQ <sub>0.8</sub>    | <b>1.09</b> | 1.11              | <b>1.09</b> |
|              | sQ <sub>0.9</sub>    | 1.16        | 1.14              | <b>1.13</b> |
|              | sQ <sub>0.95</sub>   | <b>1.22</b> | <b>1.19</b>       | <b>1.19</b> |
|              | sQ <sub>0.99</sub>   | 1.73        | <b>1.60</b>       | <b>1.59</b> |
|              | SRPS <sub>0.5+</sub> | <b>1.10</b> | <b>1.11</b>       | <b>1.10</b> |
|              | RMSSE                | <b>0.61</b> | <b>0.61</b>       | <b>0.61</b> |
| RAF          | sQ <sub>0.5</sub>    | 1.02        | 1.03              | <b>1.00</b> |
|              | sQ <sub>0.8</sub>    | 1.10        | 1.15              | <b>1.01</b> |
|              | sQ <sub>0.9</sub>    | 1.23        | 1.20              | <b>1.14</b> |
|              | sQ <sub>0.95</sub>   | 1.36        | 1.27              | <b>1.26</b> |
|              | sQ <sub>0.99</sub>   | 2.43        | 2.26              | <b>2.09</b> |
|              | SRPS <sub>0.5+</sub> | 1.15        | 1.18              | <b>1.08</b> |
|              | RMSSE                | 0.62        | <b>0.61</b>       | <b>0.60</b> |

Table 4: Comparison of GP model with different likelihoods; all models use the RBF kernel.

comparison between local and global models on intermittent time series to future works.

Our GP model uses only a RBF kernel; in future works, we could add also a periodic kernel to model the effect of seasonality, which is an open problem in intermittent time series (Fildes et al., 2022). Adding a periodic kernel to the RBF already proved to be successful in smooth time series (Corani et al., 2021).

## References

- Angelopoulos, A.N., Bates, S., 2023. Conformal prediction: A gentle introduction. *Foundations and Trends in Machine Learning* 16, 494–591.
- Athanasopoulos, G., Kourentzes, N., 2023. On the evaluation of hierarchical forecasts. *International Journal of Forecasting* 39, 1502–1511.
- Babai, M.Z., Chen, H., Syntetos, A.A., Lengu, D., 2021. A compound-Poisson Bayesian approach for spare parts inventory forecasting. *International Journal of Production Economics* 232, 107954.
- Boylan, J., Syntetos, A., 2006. Accuracy and accuracy-implication metrics for intermittent demand. *Foresight: The International Journal of Applied Forecasting* 4, 39–42.
- Boylan, J.E., Syntetos, A.A., 2021. *Intermittent demand forecasting: Context, methods and applications*. John Wiley & Sons.
- Bracher, J., Ray, E.L., Gneiting, T., Reich, N.G., 2021. Evaluating epidemic forecasts in an interval format. *PLOS Computational Biology* 17, e1008618.
- Chapados, N., 2014. Effective Bayesian modeling of groups of related count time series, in: *Proc. of the 31st International Conference on Machine Learning*, pp. II–1395.
- Corani, G., Benavoli, A., Zaffalon, M., 2021. Time series forecasting with gaussian processes needs priors, in: *Machine Learning and Knowledge Discovery in Databases. Applied Data Science Track*, Springer International Publishing, Cham. p. 103–117.
- Croston, J.D., 1972. Forecasting and stock control for intermittent demands. *Operational Research Quarterly (1970-1977)* 23, 289.
- Czado, C., Gneiting, T., Held, L., 2009. Predictive model assessment for count data. *Biometrics* 65, 1254–1261.
- Dunn, P.K., Smyth, G.K., 2005. Series evaluation of Tweedie exponential dispersion model densities. *Statistics and Computing* 15, 267–280.
- Fildes, R., Ma, S., Kolassa, S., 2022. Retail forecasting: Research and practice. *International Journal of Forecasting* 38, 1283–1318. Special Issue: M5 competition.

- Gardner, J., Pleiss, G., Weinberger, K.Q., Bindel, D., Wilson, A.G., 2018. GPyTorch: Blackbox matrix-matrix Gaussian Process inference with GPU acceleration, in: *Advances in Neural Information Processing Systems*, Curran Associates, Inc.
- Garza, F., Mergenthaler Canseco, M., Challú, C., Olivares, K.G., 2022. StatsForecast: Lightning fast forecasting with statistical and econometric models. PyCon Salt Lake City, Utah, US.
- Gelman, A., Hill, J., Vehtari, A., 2020. *Regression and Other Stories. Analytical Methods for Social Research*, Cambridge University Press.
- Gneiting, T., Raftery, A.E., 2007. Strictly proper scoring rules, prediction, and estimation. *Journal of the American Statistical Association* 102, 359–378.
- Harvey, A.C., Fernandes, C., 1989. Time series models for count or qualitative observations. *Journal of Business & Economic Statistics* 7, 407–417.
- Hastie, T., Tibshirani, R., Friedman, J.H., 2009. *The Elements of Statistical Learning: Data Mining, Inference, and Prediction*. 2nd ed., Springer.
- Hensman, J., Fusi, N., Lawrence, N.D., 2013. Gaussian Processes for big data, in: *Proceedings of the Twenty-Ninth Conference on Uncertainty in Artificial Intelligence*, AUAI Press. p. 282–290.
- Hensman, J., Matthews, A., Ghahramani, Z., 2015. Scalable variational Gaussian Process classification, in: *Proceedings of the Eighteenth International Conference on Artificial Intelligence and Statistics*, PMLR. p. 351–360.
- Hyndman, R., Koehler, A., Ord, K., Snyder, R., 2008. *Forecasting with Exponential Smoothing: The State Space Approach*. Springer Series in Statistics Series, Springer Berlin / Heidelberg, Berlin, Heidelberg.
- Hyndman, R.J., 2023. expsmooth: Data sets from "Exponential smoothing: a state space approach" by Hyndman, Koehler, Ord and Snyder (Springer, 2008). R package version 2.4.
- Hyndman, R.J., Koehler, A.B., 2006. Another look at measures of forecast accuracy. *International Journal of Forecasting* 22, 679–688.
- Januschowski, T., Wang, Y., Torkkola, K., Erkkilä, T., Hasson, H., Gasthaus, J., 2022. Forecasting with trees. *International Journal of Forecasting* 38, 1473–1481.
- Jeon, Y., Seong, S., 2022. Robust recurrent network model for intermittent time-series forecasting. *International Journal of Forecasting* 38, 1415–1425.
- Kingma, D.P., Ba, J., 2017. Adam: a method for stochastic optimization. *arXiv cs.LG. arXiv:1412.6980*.

- Kolassa, S., 2016. Evaluating predictive count data distributions in retail sales forecasting. *International Journal of Forecasting* 32, 788–803.
- Kolassa, S., 2020. Why the “best” point forecast depends on the error or accuracy measure. *International Journal of Forecasting* 36, 208–211.
- Makridakis, S., Spiliotis, E., Assimakopoulos, V., 2022. M5 accuracy competition: Results, findings, and conclusions. *International Journal of Forecasting* 38, 1346–1364.
- Nikolopoulos, K., Syntetos, A.A., Boylan, J.E., Petropoulos, F., Assimakopoulos, V., 2011. An aggregate–disaggregate intermittent demand approach (ADIDA) to forecasting: An empirical proposition and analysis. *Journal of the Operational Research Society* 62, 544–554.
- Paszke, A., Gross, S., Massa, F., Lerer, A., Bradbury, J., Chanan, G., Killeen, T., Lin, Z., Gimelshein, N., Antiga, L., Desmaison, A., Kopf, A., Yang, E., DeVito, Z., Raison, M., Tejani, A., Chilamkurthy, S., Steiner, B., Fang, L., Bai, J., Chintala, S., 2019. Pytorch: An imperative style, high-performance deep learning library, in: *Advances in Neural Information Processing Systems*, Curran Associates, Inc.
- Petropoulos, F., Kourentzes, N., 2015. Forecast combinations for intermittent demand. *Journal of the Operational Research Society* 66, 914–924.
- Prak, D., Teunter, R., 2019. A general method for addressing forecasting uncertainty in inventory models. *International Journal of Forecasting* 35, 224–238.
- Rasmussen, C.E., Williams, C.K.I., 2006. *Gaussian Processes for Machine Learning*. The MIT Press.
- Roberts, S., Osborne, M., Ebden, M., Reece, S., Gibson, N., Aigrain, S., 2013. Gaussian Processes for time-series modelling. *Philosophical Transactions of the Royal Society A: Mathematical, Physical and Engineering Sciences* 371, 20110550.
- Salinas, D., Flunkert, V., Gasthaus, J., Januschowski, T., 2020. DeepAR: Probabilistic forecasting with autoregressive recurrent networks. *International Journal of Forecasting* 36, 1181–1191.
- Saul, A.D., Hensman, J., Vehtari, A., Lawrence, N.D., 2016. Chained gaussian processes, in: *Proceedings of the 19th International Conference on Artificial Intelligence and Statistics*, PMLR. pp. 1431–1440.
- Sbrana, G., 2023. Modelling intermittent time series and forecasting COVID-19 spread in the USA. *Journal of the Operational Research Society* 74, 465–475.
- Snyder, R.D., Ord, J.K., Beaumont, A., 2012. Forecasting the intermittent demand for slow-moving inventories: A modelling approach. *International Journal of Forecasting* 28, 485–496.

- Svetunkov, I., 2024. smooth: Forecasting Using State Space Models. R package version 4.0.2.
- Svetunkov, I., Boylan, J.E., 2023. iETS: State space model for intermittent demand forecasting. *International Journal of Production Economics* 265, 109013.
- Syntetos, A.A., Boylan, J.E., 2005. The accuracy of intermittent demand estimates. *International Journal of Forecasting* 21, 303–314.
- Syntetos, A.A., Boylan, J.E., Croston, J.D., 2005. On the categorization of demand patterns. *Journal of the Operational Research Society* 56, 495–503.
- Teunter, R.H., Syntetos, A.A., Babai, M.Z., 2011. Intermittent demand: Linking forecasting to inventory obsolescence. *European Journal of Operational Research* 214, 606–615.
- Türkmen, A.C., Januschowski, T., Wang, Y., Cemgil, A.T., 2021. Forecasting intermittent and sparse time series: A unified probabilistic framework via deep renewal processes. *PLOS ONE* 16, 1–26.
- Wang, S., Kang, Y., Petropoulos, F., 2025. Combining probabilistic forecasts of intermittent demand. *European Journal of Operational Research*, S0377221724000511.
- Willemain, T.R., Smart, C.N., Schwarz, H.F., 2004. A new approach to forecasting intermittent demand for service parts inventories. *International Journal of Forecasting* 20, 375–387.
- Yelland, P.M., 2009. Bayesian forecasting for low-count time series using state-space models: An empirical evaluation for inventory management. *International Journal of Production Economics* 118, 95–103.

## Appendix A. Learning a sparse variational GP

Recall that our forecasting model learns the posterior of the latent function  $\mathbf{f}_{1:T}$  given the observations. The prior for a latent vector of length  $T$  (training data length) is  $p(\mathbf{f}_{1:T}) = \mathcal{N}(\mathbf{f}_{1:T} \mid \mathbf{0}, K_{T,T})$  and the joint distribution of data and latent variables is

$$p(\mathbf{y}_{1:T}, \mathbf{f}_{1:T}) = \prod_{i=1}^T p_{\text{lik}}(y_i; \text{softplus}(f_i), \boldsymbol{\theta}_{\text{lik}}) \mathcal{N}(\mathbf{f}_{1:T} \mid \mathbf{0}, K_{T,T}) \quad (\text{A.1})$$

The posterior over latent function  $p(\mathbf{f}_{1:T} \mid y_{1:T})$  is not available analytically therefore we need to approximate it. Moreover, in order to optimise the hyper-parameters of the model, we also need to approximate the marginal likelihood  $p(\mathbf{y}_{1:T})$ . We follow Hensman et al. (2015) and use a sparse GP model with inducing points.

We proceed by augmenting our GP model with additional  $m$  input-output pairs  $\mathbf{Z}, \mathbf{u}$  that are distributed as the GP  $f$ , i.e. the joint distribution of the vector  $(\mathbf{f}_{1:T}, \mathbf{u})$  is

$$p(\mathbf{f}_{1:T}, \mathbf{u}) = \mathcal{N} \left( \begin{bmatrix} \mathbf{f}_{1:T} \\ \mathbf{u} \end{bmatrix} \mid \mathbf{0}, \begin{bmatrix} K_{T,T} & K_{T,m} \\ K_{m,T} & K_{m,m} \end{bmatrix} \right),$$

where  $K_{m,m}$  and  $K_{T,m}$  are the covariance matrices resulting from evaluating the kernel  $k$  at the input values. Note that the Gaussian assumption implies that  $p(\mathbf{f}_{1:T} \mid \mathbf{u})$  is available analytically via Gaussian conditioning.

The joint distribution of data and latent variables thus becomes  $p(\mathbf{y}_{1:T}, \mathbf{f}_{1:T}, \mathbf{u}) = p(\mathbf{y}_{1:T} \mid \mathbf{f}_{1:T}) p(\mathbf{f}_{1:T} \mid \mathbf{u}) p(\mathbf{u})$ . We consider the approximate distribution  $q(\mathbf{u}) = \mathcal{N}(\mathbf{u} \mid \mathbf{m}, \mathbf{S})$ , where  $\mathbf{m}, \mathbf{S}$  are free parameters to be optimized.

In variational inference we assume that the posterior is approximated by  $p(\mathbf{f}_{1:T} \mid \mathbf{y}_{1:T}) \approx q(\mathbf{f}_{1:T} \mid \mathbf{y}_{1:T}) = \int p(\mathbf{f}_{1:T} \mid \mathbf{u}) q(\mathbf{u}) d\mathbf{u}$ . Since  $q(\mathbf{u})$  is Gaussian we can solve the integral analytically. We can then bound the marginal log-likelihood  $\log p(\mathbf{y}_{1:T})$  with the standard variational bound (Hensman et al., 2013)

$$\log p(\mathbf{y}_{1:T}) \geq \mathbb{E}_{q(\mathbf{u})} [\log p(\mathbf{y}_{1:T} \mid \mathbf{u})] - \text{KL}[q(\mathbf{u}) \mid p(\mathbf{u})],$$

which can be further bounded as

$$\log p(\mathbf{y}_{1:T}) \geq \mathbb{E}_{q(\mathbf{f})} [\log p(\mathbf{y}_{1:T} \mid \mathbf{f})] - \text{KL}[q(\mathbf{u}) \mid p(\mathbf{u})]. \quad (\text{A.2})$$

The right-hand side of eq. (A.2) is the evidence lower bound (ELBO). This is a loss function that can be used to optimize the model hyper-parameters  $(c, \ell, \sigma^2, \boldsymbol{\theta}_{\text{lik}})$ , the location of the inducing points  $(\mathbf{Z})$  and the variational parameters  $(\mathbf{m}, \mathbf{S})$ .

The KL part of the ELBO is available analytically, however the expectation part needs an implementation of the log-likelihood function. The expectation is then evaluated with Monte Carlo sampling by exploiting the fact that  $q(\mathbf{f})$  is a Gaussian distribution with known parameters.

We implemented the log-likelihood function  $\log p(\mathbf{y}_{1:T} \mid \mathbf{f})$  for the Tweedie likelihood and then used GPyTorch (Gardner et al., 2018) for optimizing the ELBO.

Given the optimized variational posterior approximation  $q(\mathbf{f}_{1:T} \mid \mathbf{y}_{1:T})$ , we can compute the predictive latent distribution  $h$ -step ahead as

$$p(\mathbf{f}_{T+1:T+h}) = \int p(\mathbf{f}_{T+1:T+h} \mid \mathbf{f}_{1:T}) q(\mathbf{f}_{1:T} \mid \mathbf{y}_{1:T}) d\mathbf{f}_{1:T}, \quad (\text{A.3})$$

note that this integral has an analytic solution because the distributions are both Gaussian therefore  $\mathbf{f}_{T+1:T+h}$  is a multivariate Gaussian distribution with known mean and covariance; see, e.g., Hensman et al. (2015) for detailed formulas.

The predictive posterior for the observations is computed by drawing samples  $\tilde{\mathbf{f}}^{(j)}$ ,  $j = 1, \dots, N$ , from the distribution in eq. (A.3). For each sample  $\tilde{\mathbf{f}}^{(j)}$ , we draw one sample from

$$p(\mathbf{y}_{T+1:T+h} \mid \tilde{\mathbf{f}}_{T+1:T+h}^{(j)}) = \prod_{i=T+1}^{T+h} p_{\text{lik}}\left(y_i; \text{softplus}(\tilde{f}_i^{(j)}), \boldsymbol{\theta}_{\text{lik}}\right) \quad (\text{A.4})$$

to obtain a sample from the predictive posterior. This procedure is applied for NegBinGP and TweedieGP by plugging in eq. (A.1) and (A.4) the appropriate likelihoods and parameters from Sec. 3.1 and Sec. 3.2 respectively.

In our experiments we choose the number of inducing points as follows. On short time series ( $T \leq 200$ ), we use  $T$  inducing points and initialize their locations in correspondence of the training inputs. On longer time series ( $T > 200$ ) we use 200 inducing points, sampling their initial locations from a multinomial distribution with  $p(i) \propto \log(1 + \frac{i}{T})$ ,  $i = 1, \dots, T$ . Thus the recent observations, which are more relevant for forecasting, have higher probability of being chosen as initial location of the inducing points. Since the method has a quadratic cost in  $m$ , the number of inducing points, and it is linear in  $T$ , the size of the training set, then we achieve quadratic cost in  $T$  for  $T < 200$  and linear cost in  $T$  for  $T > 200$ .

## Appendix B. Evaluation of the Tweedie density

### Appendix B.1. Truncating the infinite summation

In Sec. 3.2 we show that, given  $\mu > 0$ ,  $\phi > 0$  and  $\rho \in (1, 2)$  the Tweedie density is

$$p(y \mid \mu, \phi, \rho) = \begin{cases} \exp(-\frac{\mu^{2-\rho}}{\phi(2-\rho)}) & \text{if } y = 0; \\ A(y) \cdot \exp\left[\frac{1}{\phi} \left(y \frac{\mu^{1-\rho}}{1-\rho} - \frac{\mu^{2-\rho}}{2-\rho}\right)\right] & \text{otherwise} \end{cases} \quad (\text{B.1})$$



where

$$\begin{aligned} A(y) &= \frac{1}{y} \sum_{j=1}^{\infty} \frac{y^{j\alpha} (\rho - 1)^{-j\alpha}}{\phi^{j(1+\alpha)} (2 - \rho)^j j! \Gamma(j\alpha)} \\ &= \frac{1}{y} \sum_{j=1}^{\infty} V(j) \quad \text{with } \alpha = \frac{2 - \rho}{\rho - 1} \end{aligned} \quad (\text{B.2})$$

Dunn and Smyth (2005) evaluate  $A(y)$  by approximating the infinite sum in eq. (B.2) with a finite one, retaining its largest elements. We start by finding

$$j_{\max} = \arg \max_{j \in \mathbb{N}} V(j),$$

which is the index of the largest component. To identify it, let

$$z = \frac{y^\alpha (\rho - 1)^{-\alpha}}{\phi^{1+\alpha} (2 - \rho)}, \quad (\text{B.3})$$

then

$$V(j) = \frac{z^j}{j! \Gamma(\alpha j)}$$

and

$$\log V(j) = j \log z - \log \Gamma(1 + j) - \log \Gamma(\alpha j). \quad (\text{B.4})$$

Stirling's approximation allows us to simplify the evaluation of the Gamma function:  $\Gamma(x + 1) \simeq \sqrt{2\pi x} \cdot x^x \cdot e^{-x}$ . Therefore

$$\log \Gamma(x + 1) \simeq \frac{1}{2} \log 2\pi + \frac{1}{2} \log x + x \log x - x. \quad (\text{B.5})$$

Approximating  $\Gamma(\alpha j)$  with  $\Gamma(1 + \alpha j)$  in eq. (B.4) and using eq. (B.5) we have

$$\log V(j) \simeq j \log z - \frac{1}{2} \log 2\pi - \frac{1}{2} \log j - j \log j + j - \frac{1}{2} \log 2\pi \quad (\text{B.6})$$

$$\begin{aligned} &- \frac{1}{2} \log \alpha - \frac{1}{2} \log j - \alpha j \log \alpha - \alpha j \log j + \alpha j \\ &= j (\log z + (1 + \alpha) - \alpha \log \alpha - (1 + \alpha) \log j) \end{aligned} \quad (\text{B.7})$$

$$- \log 2\pi - \frac{1}{2} \log \alpha - \log j. \quad (\text{B.8})$$

Differentiating with respect to  $j$  we have

$$\begin{aligned} \frac{\partial \log V(j)}{\partial j} &\simeq \log z + (1 + \alpha) - \alpha \log \alpha - (1 + \alpha) \log j - j(1 + \alpha) \frac{1}{j} - \frac{1}{j} \\ &= \log z - \log j - \alpha \log(\alpha j) - \frac{1}{j} \\ &\simeq \log z - \log j - \alpha \log(\alpha j) \end{aligned} \quad (\text{B.9})$$

which is a monotone decreasing function of  $j$ . For this reason,  $\log V$  is a convex function (and therefore  $V$  too). To identify its maximum point, we equate it to 0 obtaining

$$(1 + \alpha) \log j_{\max} = \log z - \alpha \log \alpha \quad (\text{B.10})$$

and substituting  $z$  from eq. (B.3) and  $\alpha$  from eq. (B.2)

$$j_{\max}^{1+\alpha} = \frac{y^\alpha (\rho - 1)^{-\alpha}}{\phi^{1+\alpha} (2 - \rho)} \cdot \frac{(2 - \rho)^{-\alpha}}{(\rho - 1)^{-\alpha}}$$

and finally, since  $\frac{\alpha}{1+\alpha} = 2 - \rho$ :

$$j_{\max} = \frac{y^{2-\rho}}{\phi(2-\rho)}, \quad (\text{B.11})$$

where it can be appropriately rounded to be a natural number. Substituting  $j_{\max}$  into  $V$  using eq. (B.10), it gives

$$\log V(j_{\max}) = j_{\max}(1 + \alpha) - \log 2\pi - \log j_{\max} - \frac{1}{2} \log \alpha \quad (\text{B.12})$$

From this point, one can start evaluating  $V(j)$  for  $j = j_{\max} + 1, j_{\max} + 2, \dots$ , until a value  $j_U$  is found, such that

$$\frac{V(j_{\max})}{V(j_U)} \geq e^{37}$$

To compute that, one can either evaluate the difference between eqs. (B.4) and (B.12) or compute, again using eq. (B.4)

$$\begin{aligned} \log V(j_{\max}) - \log V(j_U) &\simeq (j_{\max} - j_U) C_W - (j_{\max} (1 + \alpha) + 1) \log j_{\max} \\ &\quad + (j_U (1 + \alpha) + 1) \log j_U \end{aligned} \quad (\text{B.13})$$

where  $C_W = \log z + (1 + \alpha) - \alpha \log \alpha$  does not depend on  $j$ ; such expression can be computed efficiently. Similarly, one can identify  $j_L$  such that

$$\frac{V(j_{\max})}{V(j_L)} \geq e^{37}$$

going backwards to  $j_{\max} - 1, j_{\max} - 2$ , potentially stopping at  $j = 1$ . The fact that  $\log V$  is a convex function implies that the value of  $V$  decreases exponentially on both sides. Hence, the truncated part of the summation can be bounded with geometric sums:

$$\sum_{j=1}^{+\infty} V(j) - \sum_{j=j_L}^{j_U} V(j) \leq V(j_L - 1) \frac{1 - r_L^{j_L - 1}}{1 - r_L} + V(j_U + 1) \frac{1}{1 - r_U}$$

where

$$r_L = \exp \left( \frac{\partial \log V(j)}{\partial j} \right) \Big|_{j=j_L-1} \quad \text{and} \quad r_U = \exp \left( \frac{\partial \log V(j)}{\partial j} \right) \Big|_{j=j_U+1}$$

The threshold  $e^{-37}$  has been proposed since  $e^{-37} \simeq 8 \cdot 10^{-17}$  guarantees an appropriate precision using 64-bit floating points. See Dunn and Smyth (2005) for more. In practice, we are interested in computing the log-likelihood

$$\log p(y \mid \mu, \phi, \rho) = \log A(y) + \left[ \frac{1}{\phi} \left( y \frac{\mu^{1-\rho}}{1-\rho} - \frac{\mu^{2-\rho}}{2-\rho} \right) \right]$$

which similarly requires to pass  $A(y)$  through the logarithm. To efficiently implement the evaluation of  $A$ , it is sufficient to refer to eqs. (B.2), (B.4), (B.11), (B.12), and (B.13).

| $\phi$ | 0.5  |     |     |     |     | 1.0  |     |     |     |     | 2.0  |     |     |     |     | 5.0  |     |     |     |     |
|--------|------|-----|-----|-----|-----|------|-----|-----|-----|-----|------|-----|-----|-----|-----|------|-----|-----|-----|-----|
| $\rho$ | 1.01 | 1.1 | 1.2 | 1.3 | 1.5 | 1.01 | 1.1 | 1.2 | 1.3 | 1.5 | 1.01 | 1.1 | 1.2 | 1.3 | 1.5 | 1.01 | 1.1 | 1.2 | 1.3 | 1.5 |
| 0.1    | 2    | 3   | 5   | 7   | 14  | 2    | 2   | 4   | 6   | 10  | 2    | 2   | 3   | 5   | 8   | 2    | 2   | 3   | 4   | 6   |
| 0.2    | 2    | 4   | 6   | 9   | 15  | 2    | 3   | 5   | 7   | 11  | 2    | 2   | 4   | 5   | 9   | 2    | 2   | 3   | 4   | 7   |
| 0.5    | 3    | 6   | 9   | 12  | 18  | 2    | 4   | 6   | 8   | 14  | 2    | 3   | 5   | 6   | 10  | 2    | 2   | 4   | 5   | 8   |
| 0.8    | 4    | 7   | 11  | 14  | 21  | 2    | 5   | 8   | 10  | 15  | 2    | 3   | 5   | 7   | 11  | 2    | 2   | 4   | 5   | 8   |
| 1      | 5    | 9   | 12  | 14  | 21  | 3    | 6   | 9   | 11  | 16  | 2    | 4   | 6   | 8   | 12  | 2    | 3   | 4   | 6   | 9   |
| 1.5    | 5    | 10  | 14  | 17  | 24  | 4    | 7   | 9   | 12  | 18  | 2    | 5   | 7   | 9   | 14  | 2    | 3   | 5   | 6   | 9   |
| 2      | 5    | 12  | 16  | 19  | 26  | 5    | 8   | 11  | 14  | 18  | 3    | 6   | 8   | 10  | 14  | 2    | 3   | 5   | 7   | 10  |
| 5      | 7    | 19  | 24  | 27  | 33  | 6    | 12  | 16  | 18  | 23  | 5    | 9   | 11  | 13  | 17  | 2    | 5   | 7   | 8   | 11  |
| 10     | 9    | 25  | 32  | 36  | 40  | 7    | 18  | 21  | 24  | 28  | 6    | 12  | 14  | 16  | 20  | 4    | 7   | 9   | 11  | 14  |

Table B.5:  $j_U - j_L + 1$  for different choices of  $y$ ,  $\phi$  and  $\rho$ . This is the amount of terms used in the approximation of the summation. It is an increasing function with respect to  $y$  and  $\rho$ , decreasing with respect to  $\phi$ .

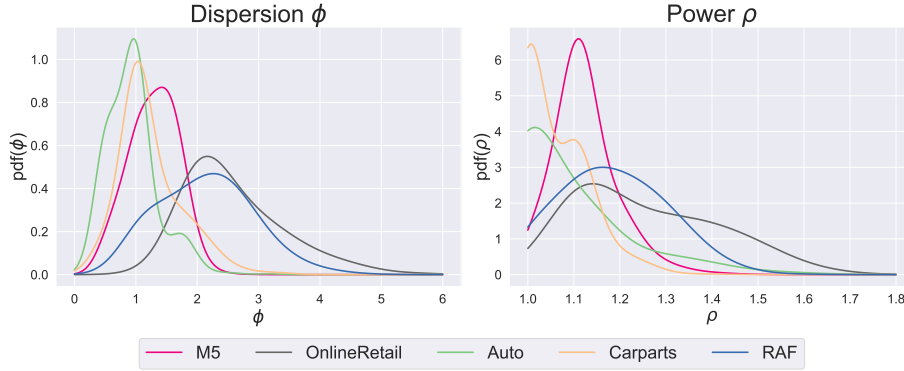


Figure B.7: The values of  $\phi$  and  $\rho$  on the fitted TweedieGP on different data sets. Density curves have been estimated via kernel density estimation.

Table B.5 shows the amount of terms in the approximation of the summation  $A$  is generally affordable; indeed scaling the data by median demand size, the value of  $y$  typically lies between 0.5 and 2, while the density plots from Fig. B.7 show that often  $\phi \in (0.5, 5)$  with mode around 1, and  $\rho \in (1, 1.4)$ , with mode around 1.1.

### Appendix B.2. Comparison with Tweedie loss

In order to consider the crucial role of  $A$  in fitting appropriately a Tweedie likelihood to the data, consider again the Tweedie loss, characterised by  $\phi = A = 1$ : in this simplified version, the implied likelihood in eq. (13) is no longer a probability distribution, as it does not integrate up to 1. If constrained to do so determining  $c := c(\mu, \phi, \rho)$  such that

$$\int_0^{+\infty} c \cdot \exp\left(y \frac{\mu^{1-\rho}}{1-\rho} - \frac{\mu^{2-\rho}}{2-\rho}\right) dy = 1$$

including the normalization constant  $c = \frac{\mu^{1-\rho}}{\rho-1} \exp\left(\frac{\mu^{2-\rho}}{2-\rho}\right)$  leads to

$$\tilde{p}(y | \mu, \rho) = \frac{\mu^{1-\rho}}{\rho-1} \exp\left(-y \frac{\mu^{1-\rho}}{\rho-1}\right),$$

which is the density function of a negative exponential distribution with parameter  $\frac{\mu^{1-\rho}}{\rho-1}$ . In this perspective, the remainder term of the loss can be interpreted as a joint prior distribution on  $\mu$  and  $\rho$  which prevents the mean from growing too large.

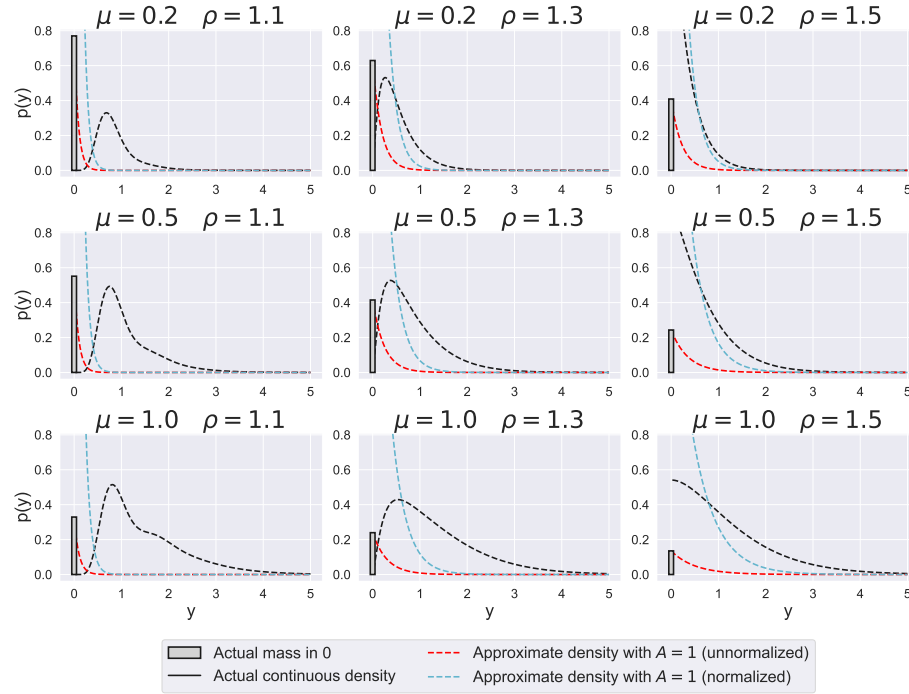


Figure B.8: In this plot,  $\phi = 1$ . In black, the Tweedie likelihood; the unnormalized density and its normalized version are the dashed lines in red and cyan respectively. The regularizing factor in the unnormalized density makes the tails shorter.

However, the resulting loss is no longer bimodal, as shown in Fig. B.8, and empirical results show that having a mass spike in zero comes with the constraint of having short tails. For this reason its performance is not satisfactory on high quantiles, despite the use of the median demand scaling.

## Appendix C. Data and code availability

All data used in the experiments is publicly available.

- M5<sup>3</sup>: this data set, released for the homonym competition (Makridakis et al., 2022), contains data from some Walmart stores.
- OnlineRetail<sup>4</sup>: this data set contains sales records of several items in an Online store. Preprocessing was required; to extract time series from tabular sales data. These are fairly long daily series. Those in which the first sale happens toward the end of the time span, although in fact smooth, may be incorrectly classified as intermittent. For this reason, time series entirely equal to zero for the first 200 timestamps were excluded.
- Auto<sup>5</sup>: short time series on automobile sales data; many of these, are not classifiable as intermittent. This data set, as well as OnlineRetail, is used by Türkmen et al. (2021).
- Carparts<sup>6</sup>: similarly to RAF, monthly time series on spare parts, but for cars. This data set is provided by Hyndman (2023).
- RAF<sup>7</sup>: this data set has been among the most widely used in the literature on intermittent series (e.g. Syntetos et al. (2005); Nikolopoulos et al. (2011); Snyder et al. (2012)). These monthly data represent the demand for spare parts for British Royal Air Force aircrafts.

The data sets are downloadable in the version used in the experiments by running first the file `datasets.R` in R and then the Python notebook `datasets.ipynb`. The files are located in the data folder at the GitHub page of the project, which will be released upon acceptance.

The code used for the experiments will be fully available at the GitHub link. The folder “tutorial” contains a simple usage example for our model.

The implementation of our GP models is based on GPyTorch (Gardner et al., 2018). Our contribution to public libraries is given by an implementation of the Tweedie class in the `distributions` module of PyTorch (Paszke et al., 2019),

---

<sup>3</sup><https://www.kaggle.com/competitions/m5-forecasting-accuracy/overview>

<sup>4</sup><https://archive.ics.uci.edu/dataset/352/online+retail>

<sup>5</sup>[https://github.com/canerturkmen/gluon-ts/tree/intermittent-datasets/datasets/intermittent\\_auto](https://github.com/canerturkmen/gluon-ts/tree/intermittent-datasets/datasets/intermittent_auto)

<sup>6</sup><https://zenodo.org/records/4656022#.YYPvWMYo-Ak>

<sup>7</sup>[https://github.com/canerturkmen/gluon-ts/tree/intermittent-datasets/datasets/intermittent\\_raf](https://github.com/canerturkmen/gluon-ts/tree/intermittent-datasets/datasets/intermittent_raf)

and the classes `TweedieLikelihood` and `NegativeBinomialLikelihood` in the `likelihoods` module of `GPyTorch`. Upon acceptance we will contribute to those packages with pull requests.

The GitHub project also contains `intermittentGP` class. It has methods to build, train and make predictions under the specification of the likelihood, the scaling and different training hyperparameters, such as the number of epochs or the learning rate of the optimizer.